Giant Zincblende Structures Formed by an ABC Star-Shaped Terpolymer/Homopolymer Blend System

Kenichi Hayashida,[†] Atsushi Takano,[†,‡] Tomonari Dotera,[§] and Yushu Matsushita*[,†]

Department of Applied Chemistry, Graduate School of Engineering, Nagoya University, Nagoya 464-8603, Japan; Precursory Research for Embryonic Science and Technology (PRESTO), Japan Science and Technology Agency, 4-1-8 Honcho, Kawaguchi 332-0012, Japan; and Department of Polymer Chemistry, Kyoto University, Kyoto 615-8510, Japan

Received June 18, 2008
Revised Manuscript Received July 23, 2008

Much attention has been focused on construction of mesoscopic diamond and/or zincblende (ZnS) structures as a result of their most robust photonic band gaps.[1−4] Self-organizing systems of spherical particles such as nanocrystal superlattices[5−8] and colloidal crystals[9−11] are candidates for building blocks of the diamond and ZnS structures. Recently, a ZnS lattice with a 19 nm lattice constant has been reported which has been obtained by fine-tuning of sizes, charges, and surface layers of nanoparticles.[7] However, it is still very difficult to construct the diamond and ZnS structures by the sphere packing plus interaction approach mainly because such structures have non-close-packed lattices.

On the other hand, it is well-known that the block copolymers exhibit a large variety of microphase-separated structures within the mesoscopic length scale in a manner that depends on the volume fractions and chain architectures of the molecules.[12−14] Among these materials, ABC star-shaped terpolymers adopt many unique microphase separations, which cannot be formed by linear-type block polymers such as AB, ABA, and ABC, in condensed[15−24] and solution[25−27] states because the three polymer chains are connected at one junction point and because the junction points must be aligned in a single dimension (Figure 1a, left). We previously reported that cylindrical structures, whose cross sections reveal various periodic tiling patterns consisting of polygons, are predominantly formed by ISP star-shaped terpolymers composed of polyisoprene (I), polystyrene (S), and poly(2-vinylpyridine) (P).[16−19] For example, the $I_1S_{1.8}P_{0.8}$ sample (Supporting Information) adopts a (6.6.6) Archimedean tiling pattern, consisting of three kinds of hexagons (Figure 1a, right).[18]

This raises the question as to what morphology is adopted by the $I_1S_{1.8}P_{0.8}$ sample when the S chains are sufficiently extended. We can imagine that if a sufficient amount of the S component surrounds the I and P chains, the junction points of the ISP star molecules will be aligned annularly (Figure 1b, left). In the microphase-separated structure, the I and P chains are inclined to form spherical domains due to the requirement of minimizing the I/S and P/S interfacial energies (Figure 1b, right). If each spherical domain is packed periodically, mesoscopic CsCl, NaCl, and/or ZnS structures can be formed by proper placement of the I and P domains alternatively. Here we report that an ISP star-shaped terpolymer/homopolymer blend system can build up a giant zincblende structure. A 3K S-homopolymer has been added to the $I_1S_{1.8}P_{0.8}$ sample to increase the volume ratio of the S component instead of extending the S chains. The resulting $I_1S_{2.3}P_{0.8}$ and $I_1S_{2.5}P_{0.8}$ samples have been found to adopt the ZnS structure. In this structure, the I and P components form spherelike domains in mutual contact at the tetrahedral positions while component S covers the I and P components as matrix.

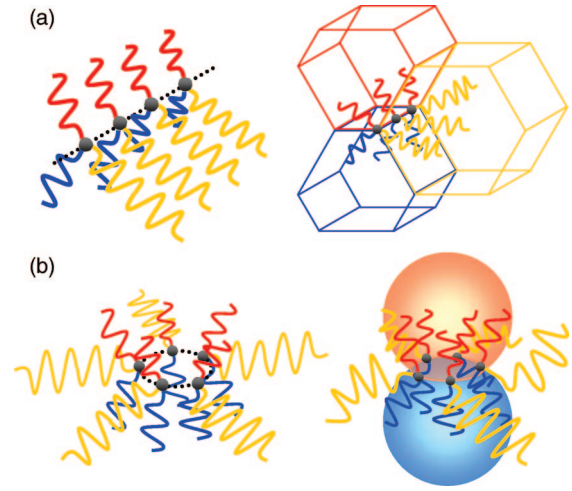

Figure 1. Schematic drawings of microphase-separated structures formed by ISP star-shaped terpolymers, composed of polyisoprene (I), polystyrene (S), and poly(2-vinylpyridine) (P) depicted in red, yellow, and blue, respectively. The illustrations on the left show two kinds of intramolecular microphase separations of ISP star-shaped terpolymer chains in bulk while the illustrations on the right indicate microdomain assembly. (a) Microphase separation with straight junction point lines. (b) Microphase separation with circle junction point lines.

Figure 2a illustrates the ZnS lattice for the $I_1S_{2.3}P_{0.8}$ sample, for which the projections of the (001) and (011) planes are simulated as shown in parts b and c of Figure 2, respectively. In these simulated projections, the contrasts among the I, S, and P components are based on transmission electron microscopy (TEM) observations. Furthermore, two TEM images of the $I_1S_{2.3}P_{0.8}$ sample in Figure 2d,e were taken with tilt angles of −20° and 25° by tilting the sample film (Supporting Information). Figure 2d shows that the I domains (black) are arranged tetragonally, suggesting that the TEM image corresponds to the (001) projections for the ZnS lattice (Figure 2b). Each P domain cannot be clearly identified in this TEM image because the S background can hardly be recognized due to the relatively larger sizes of the I and P domains in the matrix. If the sample is rotated by 45° on the *X* axis in Figure 2a, the (001) projection should be converted to (011). In our observations, the TEM image in Figure 2d was transformed into the one shown in Figure 2e by this tilting procedure. Thus, it must be an (011) image and is consistent with the (011) projection for the ZnS lattice (Figure 2c).

Crystallographic data of the ZnS structure were obtained by two types of small-angle X-ray scattering (SAXS) devices installed at two different synchrotron radiation facilities (Supporting Information). For the conventional SAXS measurement, where the size of the X-ray beam is approximately 0.4 mm × 0.7 mm (fwhm), a typical block copolymer sample provides a

* To whom all correspondence should be addressed: e-mail yushu@apchem.nagoya-u.ac.jp; Tel +81-52-789-4604; Fax +81-52-789-3210.
[†] Nagoya University.
[‡] Japan Science and Technology Agency.
[§] Kyoto University.

10.1021/ma801367v CCC: $40.75
Published on Web 08/13/2008

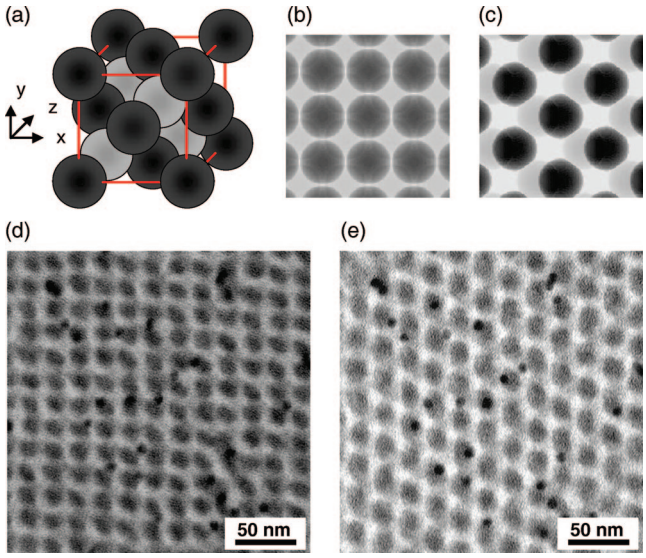

Figure 2. (a) ZnS packing model of the spherical I (black) and P (gray) domains. The radii of the I and P spheres are 0.247 and 0.232 in the unit of the lattice constant. (b, c) Simulated TEM images for the $I_1S_{2.3}P_{0.8}$ sample from the [001] (b) and [011] (c) directions of the ZnS model. (d, e) TEM images of the $I_1S_{2.3}P_{0.8}$ sample taken with tilt angles of −20° (d) and 25° (e).

powder pattern because the grains with the average size of a few microns are oriented randomly. The two curves in Figure 3a show circularly averaged SAXS intensities of the $I_{1.0}S_{2.3}P_{0.8}$ sample film for edge and through X-ray directions. Views of these curves are illustrated in the inset. The very small difference between the two SAXS profiles is indicative of nearly random orientation of the grains. In these SAXS profiles, scattering peaks located at $\sqrt{3}q/q_1 = \sqrt{3}, \sqrt{4}, \sqrt{8}, \sqrt{11}, \sqrt{12}, \sqrt{19}, \sqrt{20}, \sqrt{35}$, and $\sqrt{36}$, where q_1 is the smallest q value for the observed peaks, are identified. This is consistent with the $F\bar{4}3m$ space group symmetry of the ZnS structure. When q_1 equals $q_{\{111\}}$, the lattice constant was calculated to be 45.1 nm, which agrees well with the value of ~40 nm estimated from TEM observations (Figure 2d,e). Furthermore, a microbeam of X-rays with an approximate beam size of 5 μm × 5 μm (fwhm) was used for the second SAXS measurement. Two-dimensional SAXS patterns from the [001] and [011] directions were obtained as shown in Figure 3b because the X-ray beam size was small enough to probe only one or a few grains oriented along the same crystal axes. Owing to high resolution of the diffraction spots in the microbeam SAXS patterns, systematic extinctions are clearly observed for the $F\bar{4}3m$ space group symmetry.

The TEM and SAXS results strongly suggest that the three-dimensional structure formed by the $I_1S_{2.3}P_{0.8}$ sample is the ZnS structure. However, the observed SAXS patterns can also fit certain space group symmetries with cubic phases in addition to the $F\bar{4}3m$.[28] For example, a NaCl-type structure with $Fm\bar{3}m$ symmetry may also be formed by ISP star-shaped terpolymers. In addition, typical block copolymers tend to form double-gyroid structures consisting of two interpenetrating but nonintersecting networks in matrix components under the current conditions.[29,30] For the ISP star-polymers, these 3-connected network structures can be interpreted as representing a single network composed of alternating I and P domains contacting each other at the 3-coordinate positions.[31] Thus, three SAXS patterns were simulated for the NaCl (6-coordinate), the ZnS (4-coordinate), and the alternating gyroid (3-coordinate) structures (Supporting Information). In the simulated SAXS pattern for the NaCl model (Figure 4a, right), the intensity of the $\sqrt{4}$ peak is much weaker

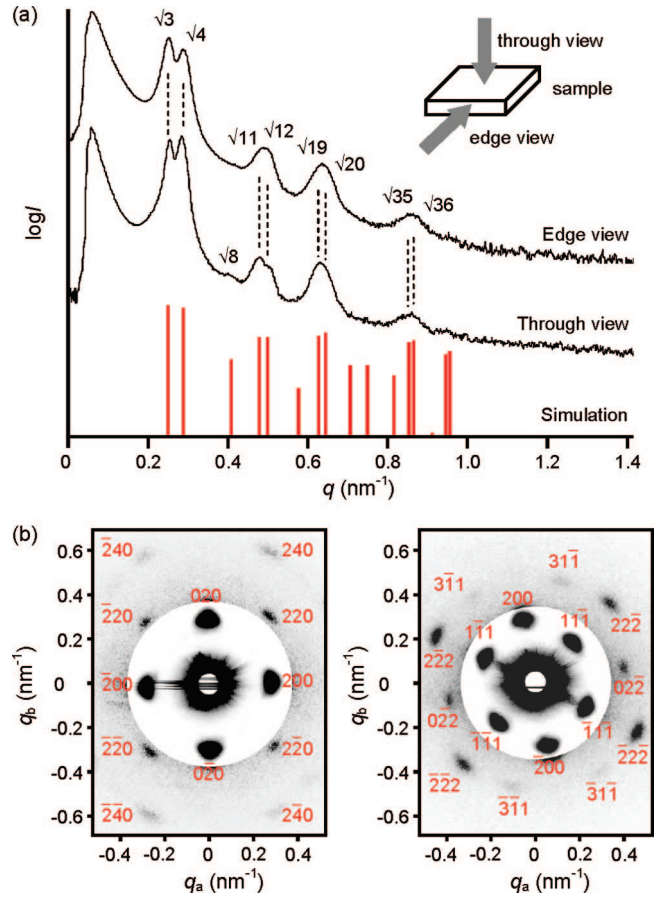

Figure 3. X-ray diffraction patterns of the $I_1S_{2.3}P_{0.8}$ sample obtained by two kinds of SAXS measurements. (a) Conventional circularly averaged SAXS profiles for edge and through views. A simulation of SAXS intensities for the ZnS-type structure is also shown at the bottom of the figure. (b) Microbeam SAXS patterns from the [001] (left) and [011] (right) directions. The intensities of the outer scattering are scaled up in these SAXS patterns.

than that of the $\sqrt{3}$ peak, which is not consistent with the experimentally determined intensities. Moreover, the simulated TEM images (Figure 4a, middle) are obviously different from the experimental TEM images (Figure 2d,e). As for the alternating gyroid structure, the peak position on the simulated SAXS pattern (Figure 4c, right) is quite different from the experimental SAXS pattern because the alternating gyroid structure is assigned to the $P4_132$ space group. On the other hand, the simulated SAXS pattern for the ZnS model (Figure 4b, right) fits quite well the experimental SAXS profiles shown in Figure 3a. Furthermore, a variation of the simulated intensities for the ZnS model is practically nothing even if the volume ratio of the $I_1S_{2.3}P_{0.8}$ sample determined by ^{1}H NMR has a significant level of error (Supporting Information).

We consider that the successful formation of the ZnS structure is a result of three predominant factors: the branched macromolecular structure, the interaction parameters among the I, S, and P components, and the volume fraction of each component for the $I_1S_{2.3}P_{0.8}$ sample. The branched molecular design makes possible the formation of the two types of spherical domains which are in contact with each other. In addition, the polymer−polymer interactions among the I, S, and P components are also important. It should be noted that the magnitude of the I/P interaction is much larger than that of the I/S and P/S interactions, or $\chi_{SI}, \chi_{SP} \ll \chi_{IP}$.[32] Consequently, the S domain tends to surround the I and P spherical domains which contact each other at relatively small surfaces to gain the I/S and P/S

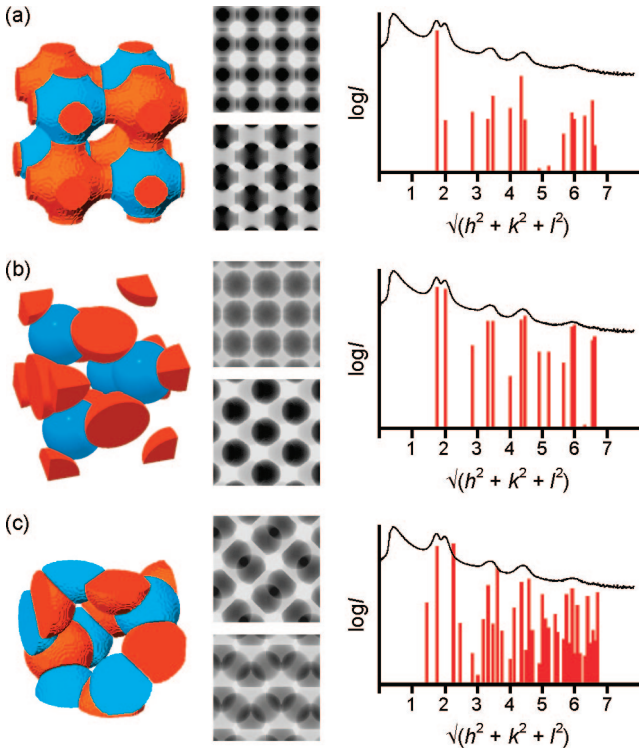

Figure 4. Conventional unit cell depictions of three different models (left column) with simulated TEM images from [001] (upper) and [011] (lower) directions (middle column) and SAXS intensities (right column). In these models, only the I and P components are depicted in red and blue, respectively. The experimental SAXS patterns for the edge view are superimposed on the simulated SAXS intensities. (a) NaCl model, (b) ZnS model, and (c) alternating gyroid model.

interfacial area instead of the I/P interfacial area. Furthermore, the reason for the advantage of the ZnS structure over the others is attributed to the volume fraction of the combined I and P components. That is, if we look for the critical volume fraction at which spheres of the two minority components can come into contact to constitute the CsCl, NaCl, ZnS, and alternating gyroid structures, the packing efficiencies are estimated to be 0.68, 0.52, 0.34, and 0.19, respectively (Supporting Information). Therefore, it is difficult for the $I_1S_{2.3}P_{0.8}$ sample to form the CsCl and NaCl structures because the total volume fraction of the I and P components for the $I_1S_{2.3}P_{0.8}$ sample is 0.45. A lower volume fraction of the I and P components might favor the alternating gyroid structure.

In conclusion, we have found a zincblende structure with a 45 nm lattice constant in an ISP star polymer system. This structure is categorized neither into bicontinuous structures nor into CsCl structures in linear ABC block polymers.[33,34] The self-assembly approach using ABC star polymers in this study is a novel attempt to build up the mesoscale non-close-packed structures.

Acknowledgment. TEM experiments were carried out under support of Dr. S. Arai and Mr. N. Saito at EcoTopia Science Institute of Nagoya University, and the authors deeply appreciate their help. Microbeam X-ray experiments were done using the machine time assigned for the Proposal No. 2007B1088 with the experimental assistance of Dr. Ohta. The authors express their thanks for this support. This work was supported by a grant from PRESTO, Japan Science and Technology Corporation (JST), and a Grant-in-Aid for Scientific Research on Priority Areas (No. 20045006) from MEXT, Japan.

Supporting Information Available: Experimental details. This material is available free of charge via the Internet at http://pubs.acs.org.

References and Notes

(1) Ho, K. M.; Chan, C. T.; Soukoulis, C. M. *Phys. Rev. Lett.* **1990**, *65*, 3152.
(2) Noda, S.; Tomoda, K.; Yamamoto, N.; Chutinan, A. *Science* **2000**, *289*, 604.
(3) Maldovan, M.; Thomas, E. L. *Nat. Mater.* **2004**, *3*, 593.
(4) Galusha, J. W.; Richey, L. R.; Gardner, J. S.; Cha, J. N.; Bartl, M. H. *Phys. Rev. E* **2008**, *77*, 050904.
(5) Bentzon, M. D.; Wonterghem, J. v.; Morup, S.; Thoelen, A.; Koch, C. J. W. *Philos. Mag. B* **1989**, *60*, 169.
(6) Redl, F. X.; Cho, K.-S.; Murray, C. B.; O'Brien, S. *Nature (London)* **2003**, *423*, 968.
(7) Kalsin, A. M.; Fialkowski, M.; Paszewski, M.; Smoukov, S. K.; Bishop, K. J. M.; Grzybowski, B. A. *Science* **2006**, *312*, 420.
(8) Abbas, S.; Lodge, T. P. *Phys. Rev. Lett.* **2006**, *97*, 097803.
(9) Hachisu, S.; Kobayashi, Y.; Kose, A. *J. Colloid Interface Sci.* **1973**, *42*, 342.
(10) Pusey, P. N.; van Megen, W. *Nature (London)* **1986**, *320*, 340.
(11) Leunissen, M. E.; Christova, C. G.; Hynniene, A.-P.; Royall, C. P.; Campbell, A. I.; Imhof, A.; Dijkstra, M.; van Roij, R.; van Blaaderen, A. *Nature (London)* **2005**, *437*, 235.
(12) Matsuo, M.; Sagae, S.; Asai, H. *Polymer* **1969**, *10*, 79.
(13) Thomas, E. L.; Anderson, D. M.; Henkee, C. S.; Hoffman, D. *Nature (London)* **1988**, *334*, 598.
(14) Bates, F. S.; Fredrickson, G. H. *Phys. Today* **1999**, *52*, 32.
(15) Hückstädt, H.; Göpfert, A.; Abetz, V. *Macromol. Chem. Phys.* **2000**, *201*, 296.
(16) Takano, A.; Wada, S.; Sato, S.; Araki, T.; Hirahara, K.; Kazama, T.; Kawahara, S.; Isono, Y.; Ohno, A.; Tanaka, N.; Matsushita, Y. *Macromolecules* **2004**, *37*, 9941.
(17) Takano, A.; Kawashima, W.; Noro, A.; Isono, Y.; Tanaka, N.; Dotera, T.; Matsushita, Y. *J. Polym. Sci., Part B: Polym. Phys.* **2005**, *43*, 2427.
(18) Hayashida, K.; Takano, A.; Arai, S.; Shinohara, Y.; Amemiya, Y.; Matsushita, Y. *Macromolecules* **2006**, *39*, 9402.
(19) Hayashida, K.; Dotera, T.; Takano, A.; Matsushita, Y. *Phys. Rev. Lett.* **2007**, *98*, 195502.
(20) Hayashida, K.; Saito, N.; Arai, S.; Takano, A.; Tanaka, N.; Matsushita, Y. *Macromolecules* **2007**, *40*, 3695.
(21) Gemma, T.; Hatano, A.; Dotera, T. *Macromolecules* **2002**, *35*, 3225.
(22) Tang, P.; Qiu, F.; Zhang, H.; Yang, Y. *J. Phys. Chem. B* **2004**, *108*, 8434.
(23) Dotera, T.; Gemma, T. *Philos. Mag.* **2006**, *86*, 1085.
(24) Huang, C.-I.; Fang, H.-K.; Lin, C.-H. *Phys. Rev. E* **2008**, *77*, 031804.
(25) Li, Z.; Kesselman, E.; Talmon, Y.; Hillmyer, M. A.; Lodge, T. P. *Science* **2004**, *306*, 98.
(26) Li, Z.; Hillmyer, M. A.; Lodge, T. P. *Macromolecules* **2006**, *39*, 765.
(27) Chou, S.-H.; Tsao, H.-K.; Sheng, Y.-J. *J. Chem. Phys.* **2006**, *125*, 194903.
(28) *F*23, $Fm\bar{3}$, *F*432, and $Fm\bar{3}m$ have the same extinction rule as $F\bar{4}3m$. Furthermore, destructive interference resulting from the form factors for the corresponding structures should be also considered for the other space groups.
(29) Hajduk, D. A.; Harper, P. E.; Gruner, S. M.; Honeker, C. C.; Kim, G.; Thomas, E. L.; Fetters, L. J. *Macromolecules* **1994**, *27*, 4063.
(30) Matsushita, Y.; Suzuki, J.; Seki, M. *Phys. B: Condens. Matter* **1998**, *248*, 238.
(31) A gyroid-type single network structure is applied to the present ISP star-shaped terpolymer system although conventional gyroid structures consist of double networks.
(32) According to recent neutron scattering experiments based on poly(isoprene-d_8-*block*-2-vinylpyridine) with M_n of 4K (by SEC) at high temperatures up to 220 °C, we were not able to reach the disordered state under the conditions employed. This result indicates that χ_{IP} is much higher than χ_{IS} and χ_{SP}.
(33) Mogi, Y.; Kotsuji, H.; Kaneko, Y.; Mori, K.; Matsushita, Y.; Noda, I. *Macromolecules* **1992**, *25*, 5408.
(34) Mogi, Y.; Mori, K.; Matsushita, Y.; Noda, I. *Macromolecules* **1992**, *25*, 5412.

MA801367V